Cocontinuous Morphologies in Polystyrene/Ethylene–Vinyl Acetate Blends: The Influence of the Processing Temperature

Ana Cristina F. Moreira, Francisco O. Cario Jr., Bluma G. Soares

Institute of Macromolecules, Federal University of Rio de Janeiro, Centro de Tecnologia, Bl J, Ilha do Fundão, 21945-970, Rio de Janeiro, RJ, Brazil

Received 13 May 2002; accepted 26 August 2002

ABSTRACT: The influence of the compression-molding temperature on the range of cocontinuity in polystyrene (PS)/ethylene–vinyl acetate (EVA) copolymer blends was studied. The blends presented a broad range of cocontinuity when compression-molded at 160°C, and they became narrower when compression-molded at higher temperatures. A coarsening effect was observed in PS/EVA (60:40 vol %) blends upon compression molding at higher temperature with an increase in the phase size of the cocontinuous structure. Concerning PS/EVA (40:60 vol %) blends, an increase in the mixing and molding temperatures resulted in a change from a cocontinuous morphology to a droplet–matrix morphology. This effect was observed by selective extraction experiments and scanning electron microscopy. The changes in the morphology with the molding conditions affected the storage modulus. An increase in the storage modulus in blends compression-molded at 160°C was observed as a result of dual-phase continuity. An EVA copolymer with a higher vinyl acetate content (28 wt %) and a higher melt-flow index resulted in blends with a broader range of cocontinuity. This effect was more pronounced in blends with lower amounts of PS, that is, when EVA formed the matrix. © 2003 Wiley Periodicals, Inc. J Appl Polym Sci 89: 386–398, 2003

Key words: morphology; blends; mechanical properties

INTRODUCTION

Polymer blends play an important role in the modern polymer industry not only for the development of new materials but also for practical recycling. It is well known that most polymers are immiscible from a thermodynamic standpoint.[1,2] Such immiscible blends exhibit different types of heterogeneous morphologies, which depend on the blend composition, interfacial tension, processing conditions, and rheological properties of the components. When one component is present in the blend at a low concentration, a dispersed phase-matrix morphology is found, for which the shape of the dispersed particles can be spherical or fibrillar.[3,4] As the concentration of the minor phase increases, particles become close enough and start to coalesce, reaching a point that corresponds to the percolation threshold point. Above this concentration, a greater and greater proportion of the minor component is incorporated into the percolation structure until at a certain volume fraction all the material of the blend components becomes part of a single percolating structure. This morphological structure is called *dual-phase continuity* or *cocontinuity*, with each phase remaining continuously connected throughout the bulk of the blend.[5–7]

Several relationships have been proposed for estimating the phase-inversion point based on the torque ratio[6–8] or viscosity ratio of the blend components,[9,10] According to these theories and empirical relationships, when the viscosities of the blend components are unequal, the low-viscosity component encapsulates the high-viscosity component and becomes the continuous phase. All these theories predict that the cocontinuous morphology is reached at only one certain value of composition. However, several experimental results have shown that this kind of morphology is not formed at a single volume fraction but can also be found over a range of volume fractions.[11–16] The range of cocontinuity depends on the interfacial tension,[13,15] the melt elasticity of the components,[7] and the molding conditions.[17]

In the range of cocontinuity, the morphologies are unstable with annealing.[11,14,16,17–20] This process may not only affect the dimensions of the phase domains but also change the range of volume fractions in which cocontinuous morphologies are found. Because the

Correspondence to: B. G. Soares (bluma@ima.ufrj.br).

Contract grant sponsor: Conselho Nacional de Desenvolvimento Científico e Tecnológico.

Contract grant sponsor: Coordenação de Aperfeiçoamento de Pessoal de Ensino Superior.

Contract grant sponsor: Fundação de Amparo à Pesquisa do Estado do Rio de Janeiro.

Contract grant sponsor: Programa de Apoio ao Desenvolvimento Científico e Tecnológico.

TABLE I
Characteristics of the Polymeric Materials

Blend component	Vinyl acetate content (wt %)	Melt flow index (g/10 min)	M_n	Torque (Nm)[a] 160°C	Torque (Nm)[a] 200°C	Interfacial tension (dyn/cm)[b] 150°C	Interfacial tension (dyn/cm)[b] 200°C	Supplier
		6.0	70,000	6.68	1.45	—	—	EDN do Brasil, Pernanbuco, Brasil
EVA18	18	2.0	55,000	5.56	3.67	—	—	Petroquimica Triunfo S.A., Rio Grande do Sul, Brasil
EVA28	28	25.0	33,000	0.93	≈0	—	—	Politeno S.A., Bahia, Brasil
PS/EVA18	—	—	—	—	—	2.8	3.2	
PS/EVA27	—	—	—	—	—	2.6	2.3	

M_n = number-average molecular weight.
[a] Torque values were obtained from a Haake internal mixer.
[b] Interfacial tension values were taken from ref. 31.

properties of polymer blends are strongly influenced by the morphology, it is possible to achieve blends with different mechanical properties at the same blend composition with different processing, such as compression or injection molding. For example, the elastic moduli of cocontinuous blends are significantly higher than the moduli of dispersed blends.[17,21] Some authors have also found an increase in the impact strength in cocontinuous blends.[22]

Cocontinuous blends also form a potential route to conductive polymer composites. When such blends are filled with conductive carbon black, this filler is homogeneously distributed inside one of the continuous phases or better yet at the interface of a cocontinuous blend.[23–26] This phenomenon gives rise to conducting materials with very low amounts of carbon black.

The aim of this article is to examine the range of cocontinuous morphologies related to polystyrene (PS)/ethylene–vinyl acetate (EVA) copolymer blends and the ways in which this range can be influenced by the compression-molding temperature and also by the characteristics of the EVA copolymer.

EVA copolymers were chosen as one of the blend components because of their unique characteristics. They impart excellent processability to polymeric materials. In addition, EVA can be obtained over a wide range of compositions. The different amounts of vinyl acetate (VA) in EVA copolymers govern the crystallinity level and thermoplastic-elastomer characteristics and may also influence the morphology and mechanical properties of the corresponding blends.

The range of cocontinuous morphologies was examined by selective extraction experiments. The coarsening process observed with compression molding at different temperatures was also investigated by scanning electron microscopy (SEM). This article also compares the cocontinuity morphology with the dynamic mechanical behavior and tensile properties for PS/EVA blends of different compositions.

EXPERIMENTAL

Materials

A general-purpose PS and two types of EVA with different vinyl acetate contents were employed in this work. The basic characteristics of these materials are listed in Table I.

Blend preparation

All blends were prepared with a Haake internal mixer (Dallas, TX) equipped with roller blades and operating at 60 rpm. PS/EVA18 and PS/EVA28 blends with different compositions were prepared at two different temperatures (160 and 200°C). PS pellets were fed into a preheated chamber. After 50 s, the EVA component was introduced, and the blend was allowed to mix for 10 min. The samples were then compression-molded in a laboratory hydraulic press for 10 min at the same blending temperature with 6 MPa of pressure. The compression-molded samples were immediately transferred to another hydraulic press equipped with a water-circulating refrigerator system to cool down the samples to room temperature under the same pressure used in the compression-molding operation.

Extraction experiments

Cocontinuity in the blends was checked by extraction experiments. The PS phase was selectively extracted for 7 days at room temperature with methyl ethyl ketone (MEK) as the solvent. This procedure was sufficient for the complete removal of the soluble fraction. The EVA phase could not be selectively extracted because the solvent that could dissolve EVA (hot toluene) also dissolved the PS phase. After the extraction with MEK, the piece of the specimen that was self-supported was taken from the solvent, dried, and weighed.

Microscopy

Samples were prepared by cryofracture in liquid nitrogen. The surface was submitted to treatment with MEK for selective extraction of the PS phase. Before microscopy analysis, the samples were coated with a thin layer of gold. A scanning electron microscope (JEOL JSM-5610LV, Tokyo, Japan) was used with an electron voltage of 20 kV and a secondary electron detector. The size and size distribution of the dispersed particles were determined by means of semiautomatic image analysis. The SEM micrograph of the fractured sample was first scanned and converted into digitized image, which was analyzed with the Analysis 3.0 program (Tokyo, Japan) to obtain the average diameter values of the dispersed particles (d_n) and the particle size distribution.

Tensile properties

Tensile experiments were performed with an Instron 4204 tensile tester (Boston, MA) at room temperature in accordance with ASTM D 638. For PS-rich blends, the crosshead speed was set at 1 mm min−1, and for EVA-rich blends, a crosshead speed corresponding to 50 mm min−1 was employed.

Dynamic mechanical measurements

Dynamic mechanical measurements were carried out on a Rheometric Scientific MKIII dynamic mechanical thermal analyzer (New Jersey). The experiments were conducted in a flexure mode at a frequency of 1 Hz. The samples (2 × 10 × 25 mm3) were heated at 2°C/min over a range of −50 to 150°C.

RESULTS AND DISCUSSION

Region of dual-phase continuity

It was our goal to study the location and width of the region of phase cocontinuity of PS/EVA blends prepared with different EVA copolymers and at different compression-molded temperature. The continuity of each phase was first determined from selective extraction experiments, which have been reported to be a very good tool for estimating the cocontinuity in heterogeneous polymer blends.[6−8] In this study, MEK was employed as a selective solvent for the PS phase. When PS is completely dispersed inside the EVA matrix, the solvent cannot reach the PS domains, and no material can be extracted. In this morphological situation, one can assume that PS is 0% continuous. With the volume fraction of PS increasing, the dispersed phase starts to coalesce and presents a certain degree of continuity. This degree corresponds to the amount of PS that can be extracted by the solvent. When both phases are continuous, the solvent can dissolve the entire PS phase without causing any disintegration of the material.

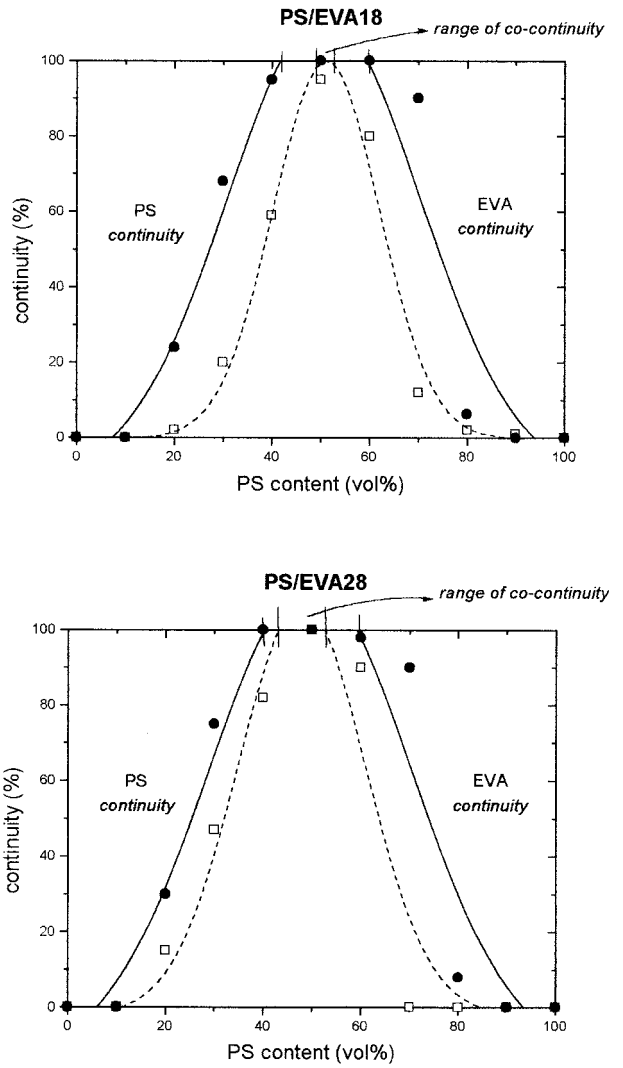

Figure 1 Continuity degree of PS and EVA phases in PS/EVA blends as a function of the blend composition. The blends were compression-molded at (●) 160 and (□) 200°C.

After a certain blend composition, the PS phase starts to be the continuous phase, and its extraction with MEK causes disintegration of the blend material; a milky solution is obtained. However, if the EVA phase presents a certain degree of continuity, the treatment with MEK will leave some pieces of the sample with a self-supported characteristic. In this case, the degree of continuity of the EVA phase can be estimated by the weighing of these self-supported pieces.

Figure 1 illustrates the change in the continuity degree of both PS and EVA phases with the blend composition as a function of temperature processing. Blends prepared at 160°C display a wide range of dual-phase continuity. When the same blends are compression-molded at 200°C, the continuity range becomes narrower, and the percolation threshold is

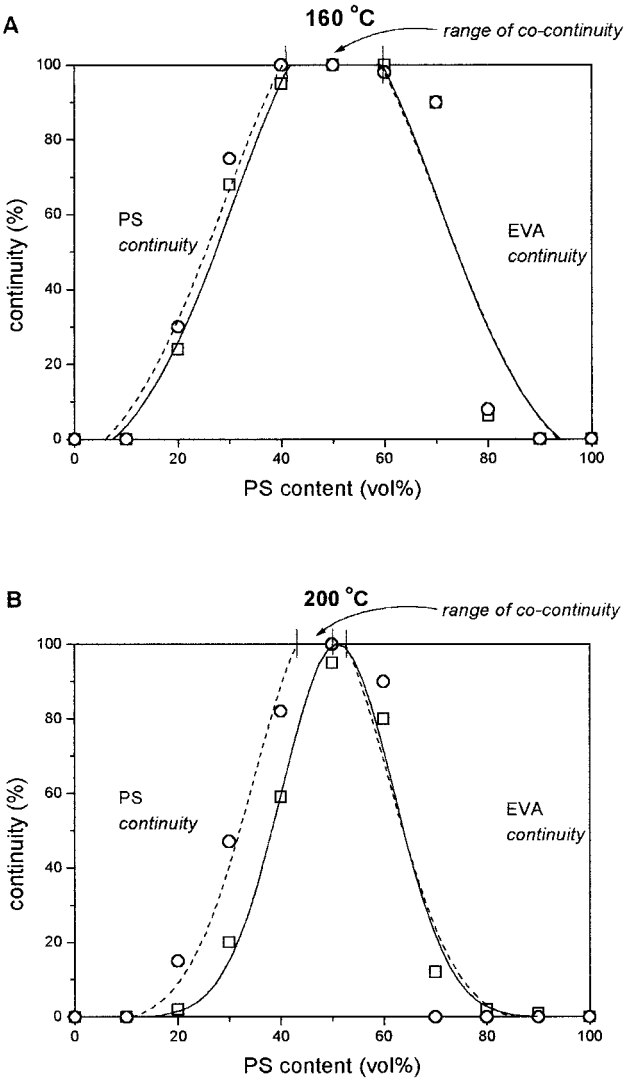

Figure 2 Effect of the EVA nature on the continuity degree of PS and EVA phases in PS/EVA blends: (□) PS/EVA18 and (○) PS/EVA28. The blends were compression-molded at (A) 160 and (B) 200°C.

shifted toward a larger amount of the minor component.

The influence of the EVA sample (EVA18 or EVA28) is more pronounced in blends with a lower amount of PS, that is, when EVA forms the matrix. This effect is shown in Figure 2. In this region, the percolation threshold point (when the dispersed PS phase starts to coalesce and shows some degree of continuity) is shifted toward a lower amount of PS when the EVA28 blend component constitutes the matrix. This effect is significant in blends prepared at 200°C.

According to the literature, the elongated structures, which form the cocontinuous morphology, are nonequilibrium states under quiescent conditions and will change form because of the interfacial tension.[16] The interfacial area tends to decrease when the blend is kept at an elevated temperature, and this results in an increase in the phase size of the cocontinuous blend or in a breakup of the cocontinuous structure into a droplet–matrix morphology. The coarsening effect on annealing or compression molding, in which the cocontinuity is still found but the dimensions of the phase are affected, can be better observed with SEM analysis. Figure 3 presents the morphologies of PS/EVA18 and PS/EVA28 blends (60:40 vol %) compression-molded at 160 and 200°C. The dark sections correspond to the PS phase selectively extracted with MEK. Blends compression-molded at 160°C display a typical cocontinuous morphology, as also indicated by extraction experiments [see Fig. 3(a,b)].

The same blends compression-molded at 200°C also maintain the cocontinuity, but the phase sizes increase substantially [see Fig. 3(c,d)]. This coarsening effect of cocontinuous morphologies in polymer blends with annealing at higher temperatures has also been reported in the literature,[14–16] and can be attributed to phase coalescence, which is favored by the interfacial tension between these immiscible blend components and also by a decrease in the flow viscosity during the molding process at higher temperatures. At this blend composition, the one compounded with the EVA28 component displays a greater coarsening process.

The morphologies of PS/EVA (40:60 vol %) blends have also been investigated as a function of the molding temperature, as illustrated in Figure 4. At this blend composition, PS constitutes the minor component, and changes in the cocontinuous structure into a droplet–matrix morphology with compression molding at higher temperatures can be observed. Both PS/EVA18 and PS/EVA28 blends with a composition corresponding to 40:60 vol % present typical cocontinuous morphologies when compression-molded at 160°C [see Fig. 4(a,b)]. This result is in agreement with selective extraction experiments.

With the molding temperature increasing to 200°C, there is a breakup of the elongated PS phase in both PS/EVA18 [Fig. 4(c)] and PS/EVA28 [Fig. 4(d)] blends, and the cocontinuous morphology changes to a droplet–matrix morphology.

The particle size distribution of the PS domains dispersed in EVA18 and EVA28 matrices related to the blends compression-molded at 200°C is shown in Figures 5 and 6, respectively. As a rule, the average size of the minor phase in polymer blends is controlled by several parameters, including the interfacial tension, torque or viscosity ratio (of the dispersed phase with respect to the matrix), and elasticity ratio.[3,27–30] It is generally accepted that the size of the minor phase in binary blends decreases with a decrease in the interfacial tension, torque ratio, and elasticity of the dispersed phase. For the systems investigated in this study, the torque ratios (Table I) allow us to predict smaller PS particle sizes for the PS/EVA18 (40:60 vol %) blend. As shown in Figure 5, this blend contains a

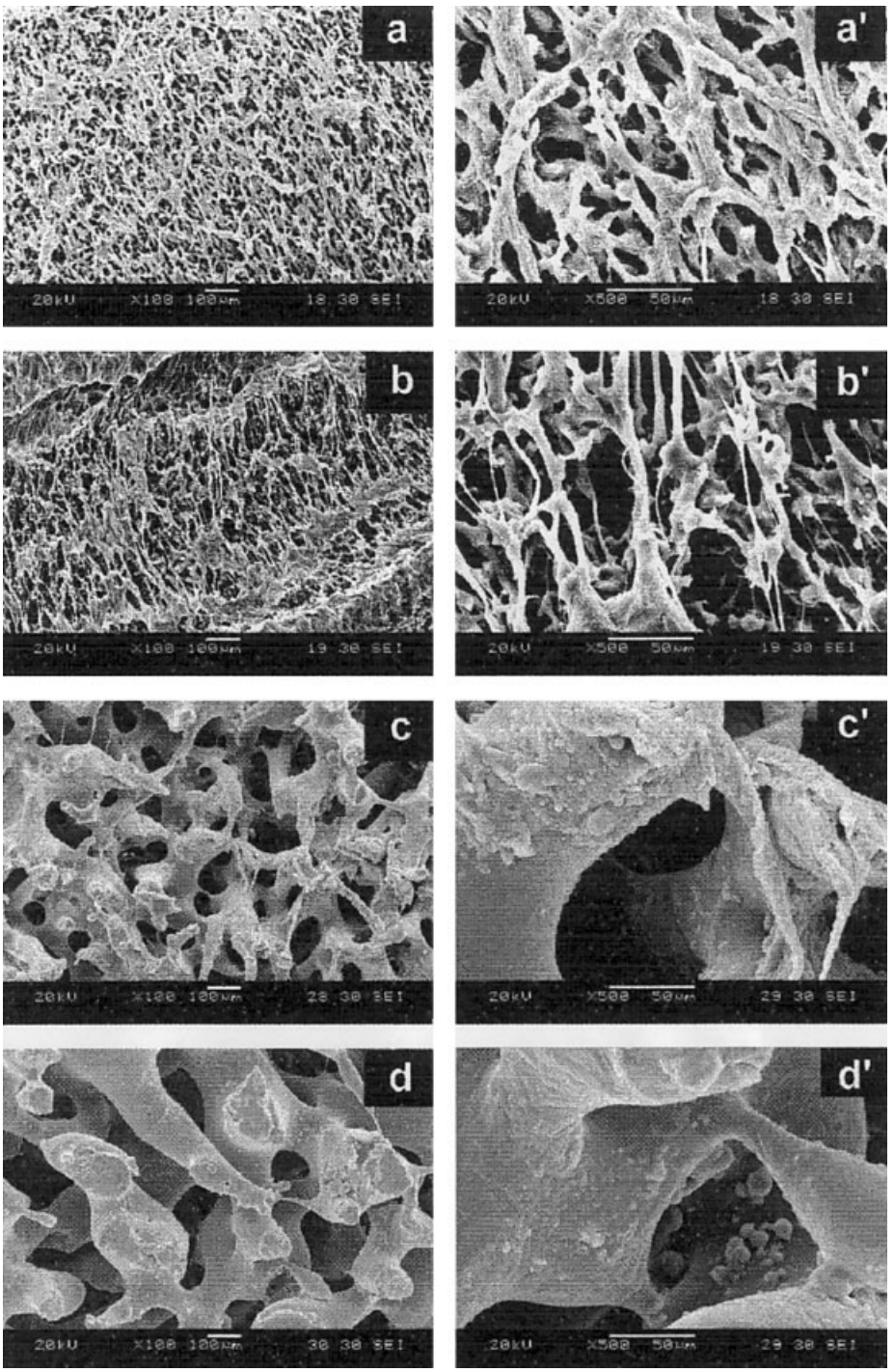

Figure 3 SEM micrographs of PS/EVA (60:40 vol %) blends: (a) PS/EVA18 and (b) PS/EVA28 compression-molded at 160°C and (c) PS/EVA18 and (d) PS/EVA28 compression-molded at 200°C (a′–d′ correspond to a–d at a higher magnification, 500×).

great number of particles about 2 μm in diameter. In the PS/EVA28 blend, the torque ratio is increased, and a bimodal particle size distribution is observed (see Fig. 6), with one set at about 2 μm and the other at about 12 μm. There is also a small number of particles around 200 μm in diameter that appear in the micrograph but are not shown in Figure 6.

According to literature data (see Table I), the interfacial tension corresponding to PS/EVA27 blends is lower than that corresponding to PS/EVA18 blends, and this difference is more accentuated when the experiment is performed at 200°C.[31] According to this parameter, one should expect a larger PS particle size when EVA18 is the matrix. However, the viscosity of

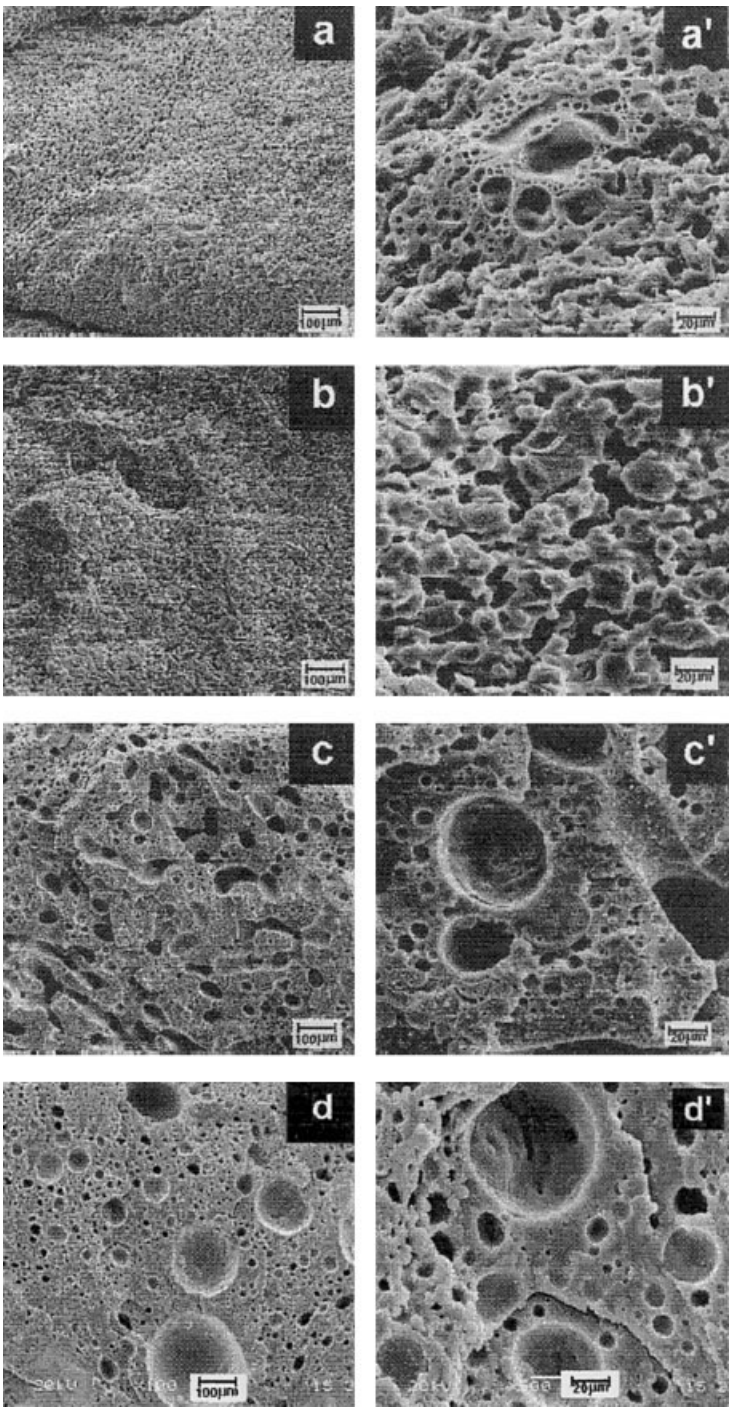

Figure 4 SEM micrographs of PS/EVA (40:60 vol %) blends: (a) PS/EVA18 and (b) PS/EVA28 compression-molded at 160°C and (c) PS/EVA18 and (d) PS/EVA28 compression-molded at 200°C (a′–d′ correspond to a–d at a higher magnification, 500×).

the EVA28 matrix is lower, and this feature can be responsible for the presence of particles as large as 200 μm in the PS/EVA28 (40:60 vol %) blend. Actually, the final morphology results from more or less complex interplay of the physical properties of the dispersed/matrix pair.

Dynamic mechanical behavior

As dynamic mechanical properties depend mainly on the nature of the matrix, dynamic mechanical thermal analysis (DMTA) results should give extra information concerning the blend composition with dual-

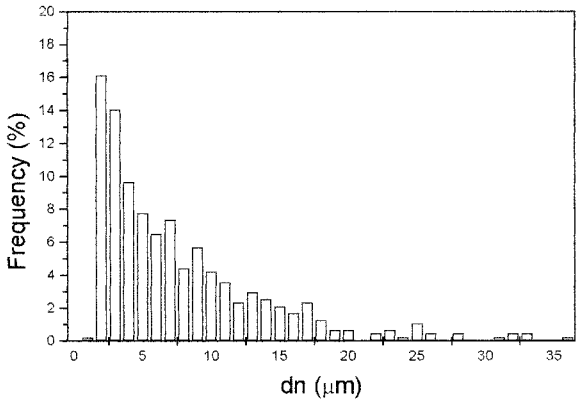

Figure 5 PS particle size distribution of a PS/EVA18 (40:60 vol %) blend prepared at 200°C.

phase continuity. The dynamic mechanical properties have been analyzed for PS/EVA18 and PS/EVA28 blends prepared at 160 and 200°C. Figure 7 illustrates the storage modulus (E') as a function of the temperature for PS/EVA18 and PS/EVA28 blends prepared at 160°C. The first decrease in E' around −25°C corresponds to the glass-transition temperature (Tg) of the amorphous part of EVA, whereas the large decrease around 90–120°C corresponds to Tg of the PS phase. The E' curve profiles change substantially with the composition. The highest differences are found in the plateau region between the two glass transitions. At this temperature range, E' decreases as the amount of EVA in the blend increases. The differences in E' values with the composition are functions of the EVA sample (EVA18 or EVA28) and must also be influenced by the blend morphology.

Several theories[17,21,32–38] have been used to relate the modulus of a multiphase system (e.g., polymer blends, composites, and interpenetrating networks) to its composition and morphology. To analyze the elastic modulus of binary blends with hard plastic and soft elastomeric components, one can employ Takayanagi's mechanical model.39 The upper bound in the modulus is obtained with the parallel model; this means that the elastic behavior at small strains is controlled by the hard phase. This corresponds to an ideal case in which the plastic component is the continuous phase and the elastomeric component is the dispersed phase. The lower bound in the modulus corresponds to the series model, in which the hard plastic phase and the soft elastomeric phase are in series. This models the case in which the soft phase is continuous:

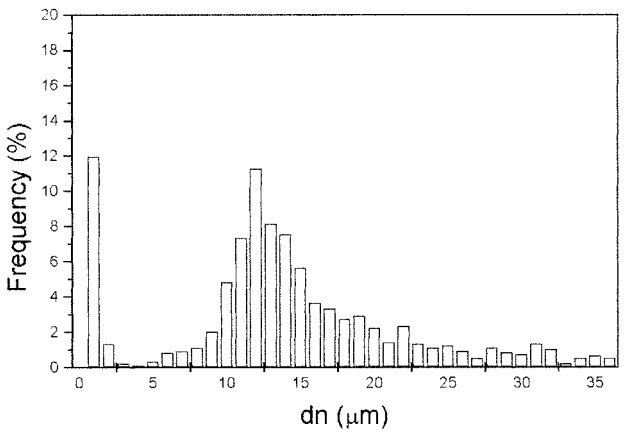

Figure 6 PS particle size distribution of a PS/EVA28 (40:60 vol %) blend prepared at 200°C.

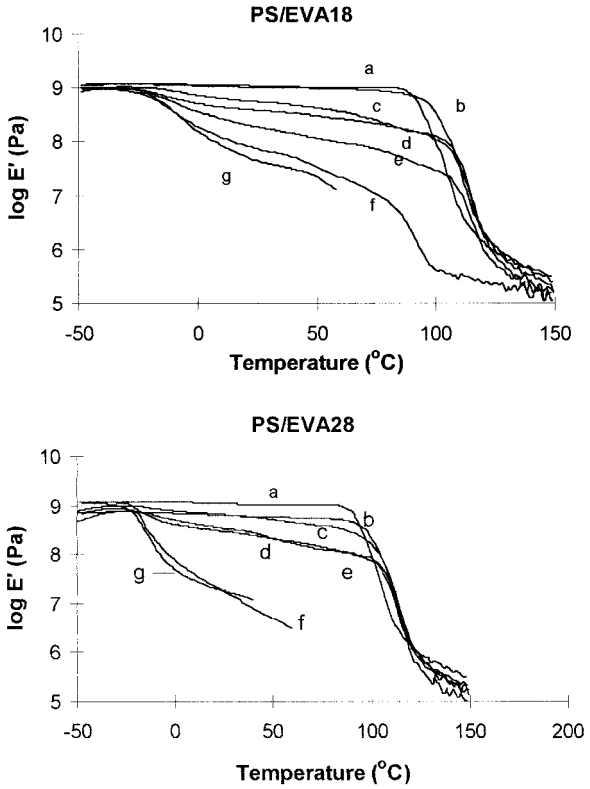

Figure 7 E' values of PS/EVA blends compression-molded at 160°C as a function of the temperature. The PS contents in the blends were (a) 100, (b) 80, (c) 60, (d) 50, (e) 40, (f) 20, and (g) 0 vol %.

$$\text{Upper bound: } E = \phi_1 E_1 + \phi_2 E_2 \quad (1)$$

$$\text{Lower bound: } E = [\phi_1/E_1 + \phi_2/E_2]^{-1} \quad (2)$$

where E, $E1$, and $E2$ are the moduli of the blend, the first blend component, and the second blend component, respectively, and ϕ is the volume fraction. These models do not include any strength of interactions between the two components.

Kerner[40] developed a model for polymer blends containing a dispersed phase consisting of spherical particles with some adhesion between the phases:

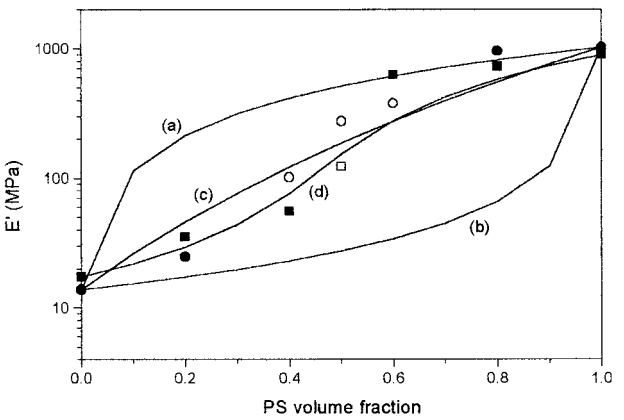

Figure 8 E' values versus the composition data for PS/EVA18 blends in comparison with modulus–composition models: (a) parallel, (b) series, (c) Davies, and (d) Budiansky. The blends were prepared at (●) 160 and (■) 200°C. The open symbols represent cocontinuous morphologies.

$$E = E_1\left[\frac{\frac{\phi_1}{15(1-\nu_1)} + \frac{\phi_2 E_2}{(7-5\nu_1)E_1 + (8-10\nu_1)E_2}}{\frac{\phi_1}{15(1-\nu_1)} + \frac{\phi_2 E_1}{(7-5\nu_1)E_1 + (8-10\nu_1)E_2}}\right] \tag{3}$$

where E, $E1$, and $E2$ are the moduli of the blend, the matrix, and the dispersed phase, respectively; $\phi 1$ and $\phi 2$ are the volume fractions of the matrix and dispersed phase, respectively; and $\nu 1$ is Poisson's ratio of the matrix. This equation can be greatly simplified in some cases. For a dispersed phase that is much more rigid than the polymer matrix, that is, $E1 \ll E2$ (e.g., in systems of rubber reinforced by carbon black), the Kerner equation simplifies to

$$E = E_1\left[1 + \frac{15(1-\nu_1)\phi_2}{2(4-5\nu_1)\phi_1}\right] \tag{4}$$

However, if the matrix is much more rigid than the dispersed phase, $E2 \ll E1$, such as in impact resistant plastics, the Kerner equation simplifies to

$$E = E_1\left[\frac{1}{1 + (15(1-\nu_1)\phi_2/(7-5\nu_1)\phi_1)}\right] \tag{5}$$

More recently, Davies[41,42] proposed a new relationship that is thought to be suitable for systems in which both phases are continuous at all concentrations, such as interpenetrating networks. He assumed that a mixture of two components, with moduli $E + \Delta E$ and $E - \Delta E$, results in a new blend or composite with E, the value of which can be determined as follows:

$$E^{1/5} = \phi_1 E_1^{1/5} + \phi_2 E_2^{1/5} \tag{6}$$

A model that predicts phase inversion at midrange compositions in two-phase polymer systems was developed by Budiansky:[43]

$$\frac{\phi_1}{1 + \varepsilon\left(\frac{G_1}{G} - 1\right)} + \frac{\phi_2}{1 + \varepsilon\left(\frac{G_2}{G} - 1\right)} = 1 \tag{7}$$

Again, ϕ is the volume fraction, ϵ equals $2(4 - 5\nu)/15(1 - \nu)$, ν is Poisson's ratio of the composite, G is the shear modulus, and subscripts 1 and 2 represent the polymer components. The conversion from G to the tensile or elastic modulus (E) was conducted with the equation $E = 2G(1 + \nu)$.[44] ν was assumed for the flexible EVA component to be 0.544 and for the PS component to be 0.33,[45] and Poisson's ratios for the compositions were calculated with the linear rule of mixing.

To analyze the storage modulus behavior according to these modulus–composition theories, we have chosen the E' values taken at an intermediate temperature (50°C) between the EVA and PS transition values. These values are plotted as a function of the PS content and compared to the values predicted with the Takayanagi [eqs. (1) and (2)], Davies , and Budiansky models in Figures 8 and 9. The open symbols in these figures represent the systems with a cocontinuous morphology, as determined by selective extraction experiments.

At higher amounts of PS (ca. 80 vol %), all blends display high values of E' because EVA is completely dispersed inside PS and the solid-state properties of the matrix dominate. At this composition, all systems are in good agreement with the parallel model [eq. (1), curve a], in which the elastic behavior is controlled by the hard phase. This morphological situation is also evident from selective extraction experiments (Fig. 1).

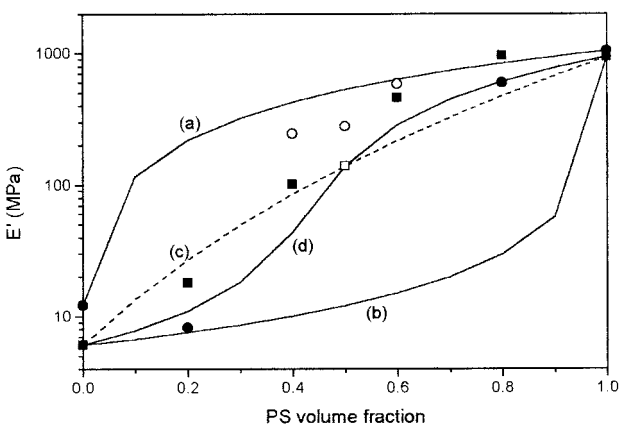

Figure 9 E' values versus the composition data for PS/EVA28 blends in comparison with modulus–composition models: (a) parallel, (b) series, (c) Davies, and (d) Budiansky. The blends were prepared at (●) 160 and (■) 200°C. The open symbols represent cocontinuous morphologies.

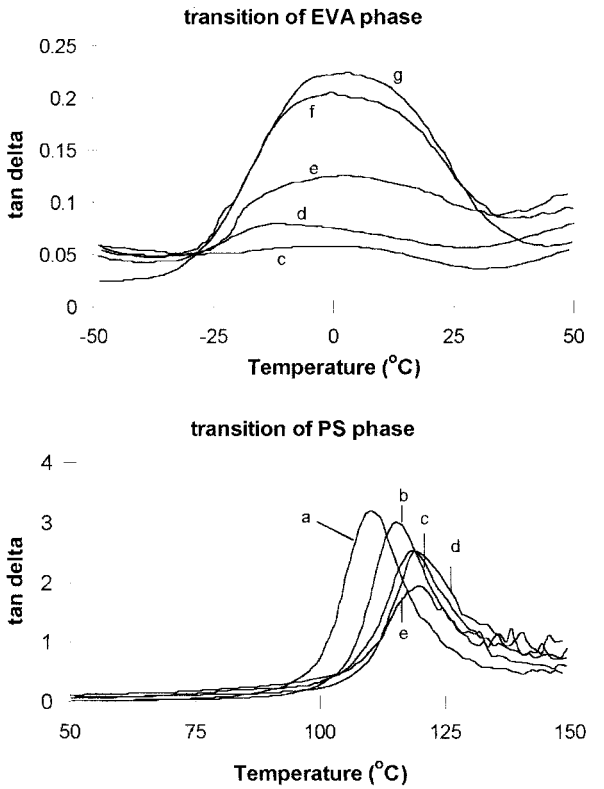

Figure 10 Tan δ values of PS/EVA18 blends compression-molded at 160°C. The PS contents in the blends were (a) 100, (b) 80, (c) 60, (d) 50, (e) 40, (f) 20, and (g) 0 vol %.

As the amount of EVA in the blend increases, the corresponding dispersed particle size starts to increase as a result of the coalescence, and the contribution of this soft phase for the E' values becomes important. Therefore, the E' values start to decrease. At a low PS volume fraction (ca. 20 vol %), the E' values of these systems are quite close to those of the series model [eq. (2), curve b].

The modulus behavior of both PS/EVA blends is also influenced by the compression-molding temperature in the composition range between 60:40 and 40:60 vol %. The PS/EVA18 blends compression-molded at 160°C exhibit a cocontinuity range from 40 to 60 vol % PS, as indicated by extraction experiments (Fig. 1) and SEM micrographs [Figs. 3(a) and 4(a)]. The moduli of these cocontinuous blends (see Fig. 8) are not as high as those predicted by the parallel model (curve a) but are very high compared with those predicted by the series model (curve b). These values are more similar to the Davies (curve c) and Budiansky (curve d) models, which take into account the phase cocontinuity. These high moduli in the cocontinuous blends, compared with those of the droplet–matrix morphology blends constituted by an EVA matrix, are attributed to a very effective stress transfer in the fully physical interpenetrating networks.

The cocontinuous range of the PS/EVA18 blends compression-molded at 200°C becomes narrow (between 50 and 55 vol % PS), as indicated by extraction experiments. The modulus at a blend composition of 50 vol % is in good agreement with the Budiansky model (curve d), which predicts the phase inversion at a midrange composition. It must be due to the differences in the phase size of the physical interpenetrating networks. For the PS/EVA18 (40:60 vol %) blend, it is interesting to observe the higher modulus of the blend compression-molded at 160°C due to the cocontinuous morphology achieved at this condition. These results are in good agreement with the SEM micrographs. As observed in Figure 4(a′), this blend displays a cocontinuous morphology when compression-molded at 160°C and changes to a droplet–matrix morphology [Fig. 4(c′)] when compression-molded at 200°C. For the PS/EVA18 (50:50 vol %) blend, the cocontinuous morphology was detected from extraction experiments under both conditions. However, the modulus of the sample compression-molded at 160°C is higher, probably because of the difference in the phase sizes of the physical interpenetrating networks.

The effect of the blend composition and compression-molding temperature on the modulus of PS/EVA28 blends is illustrated in Figure 9. The behavior is similar to those found for PS/EVA18 blends. In the range between 40 and 60 vol % PS, the blends display

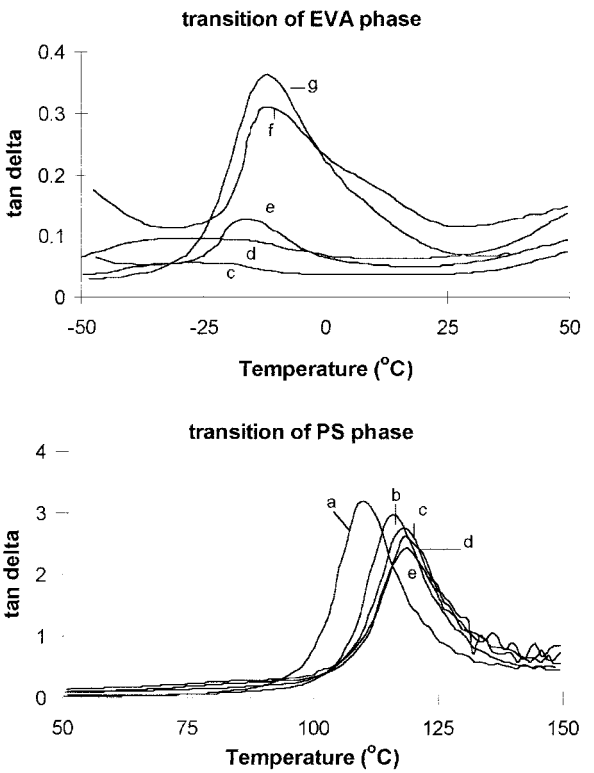

Figure 11 Tan δ values of PS/EVA28 blends compression-molded at 160°C. The PS contents in the blends were (a) 100, (b) 80, (c) 60, (d) 50, (e) 40, (f) 20, and (g) 0 vol %.

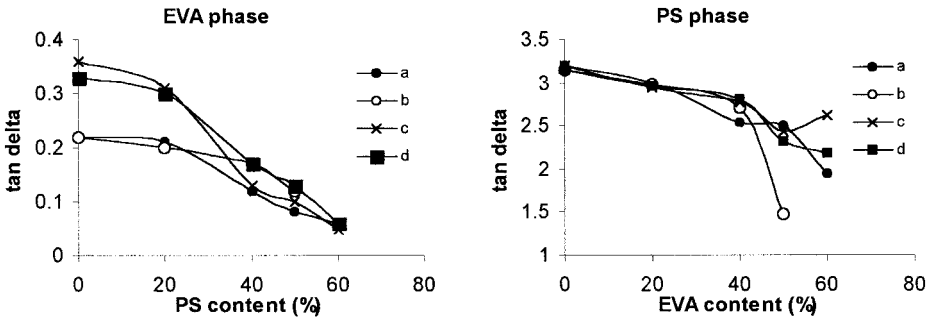

Figure 12 Tan δ values of PS/EVA blends as a function of the blend composition. PS/EVA18 was compression-molded at (a) 160 and (c) 200°C; PS/EVA28 was compression-molded at (b) 160 and (d) 200°C.

a cocontinuous morphology when compression-molded at 160°C, as indicated by extraction experiments (Fig. 1) and SEM micrographs [Figs. 3(b) and 4(b)] and present higher modulus values than those predicted by the series, Davies, or Budiansky models. These modulus behaviors can be attributed to the strong influence of the PS hard phase. Blends compression-molded at 200°C display lower moduli at this composition range. The blend containing 40 vol % PS is not cocontinuous [see Fig. 4(d)], and the modulus is influenced by the EVA matrix. The modulus of the PS/EVA28 (50:50 vol %) blend compression-molded at 200°C completely fits into the Budiansky model, indicating a narrow region of phase-inversion morphology.

The experimental data points for E' do not fit exactly into any of the theoretical models investigated. However, the shape of the Budiansky equation, involving phase inversion at the intermediate composition, gives the best approximation for blends compression-molded at 200°C. When the moduli of the cocontinuous blends are compared to those of the dispersed morphologies (with the same volume fractions), it becomes evident that the cocontinuous blends show higher values of the modulus than the dispersed blends. Figures 8 and 9 also show that the E' values of cocontinuous blends cannot be well described by the Davies model (which is based on the concept of dual-phase continuity). Some experimental values are higher than those predicted by the model , and others are lower.

Tan δ values of these blends have also been investigated. Figures 10 and 11 illustrate these results for PS/EVA18 and PS/EVA28 blends, respectively, compression-molded at 160°C. All blends display two transitions related to EVA and PS phases, as expected for incompatible blends. These blends are constituted by an amorphous component, PS, and a semicrystalline one, EVA. The tan δ value corresponding to the PS component is higher than that corresponding to the EVA component because of the amorphous nature of the former. In this sense, the EVA 28 component displays higher tan δ values than EVA18 because the crystallinity degree of the former is lower; that is, EVA28 contains a larger amount of the amorphous phase, which is responsible for this glass transition.

The maximum intensity of the tan δ peaks, corresponding to the glass transitions of both PS and EVA phases, depends not only on the volume fraction of each phase in the blend but also on the blend morphology, as reported in the literature.39,46 In Figure 12, the maximum tan δ related to EVA and PS phases is plotted as a function of the EVA content in all PS/EVA blends. Obviously, the maximum tan δ of the EVA phase decreases as the amount of this component in the blend decreases. However, this phenomenon cannot only be related to the blend composition because the variation is more pronounced beyond a certain concentration of the PS phase in the blend. In addition, blends constituted by the same components present a different dependence of tan δ with the composition when prepared at different temperatures. The drastic change in the maximum tan δ values can be related to the point of phase inversion. For PS/EVA18 blends (curves a and c), the phenomenon occurs around 20 vol % PS. A similar behavior can also be observed for the maximum tan δ of the PS phase. In this case, the discontinuity in the curves occurs around 40 vol % EVA in the blend, suggesting that this phase starts to be continuous.

The temperature corresponding to the maximum of tan δ is normally related to *Tg*. The dependence of *Tg* of both phases on the blend composition is presented in Figure 13. For blends richer in PS, *Tg* of the PS phase shifts toward higher temperatures as the amount of EVA in the blend increases, indicating a decrease in the mobility of the PS phase. This phenomenon can be explained as follows: when the glass–rubber transition of the PS phase is achieved, the EVA phase is in the rubbery state and thermally expanded. This effect causes a decrease in the free volume of the PS phase and contributes to an increase in the *Tg* values.

However, when EVA is the major component in the blend, one can find different behaviors in the *Tg* values of the EVA phase. PS/EVA28 blends compression-

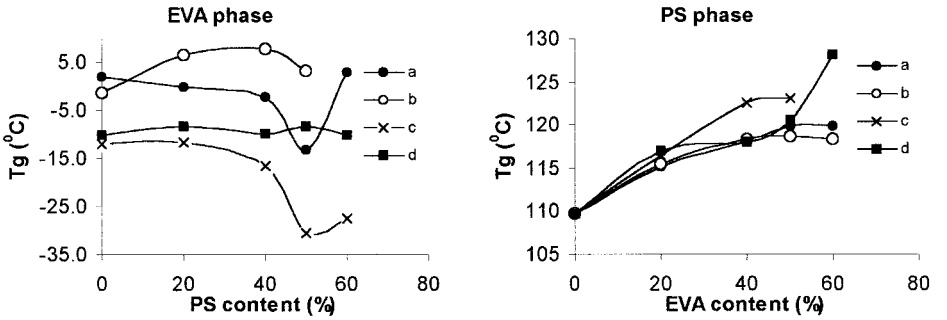

Figure 13 *Tg* of PS/EVA blends as a function of the blend composition. PS/EVA18 was compression-molded at (a) 160 and (c) 200°C; PS/EVA28 was compression-molded at (b) 160 and (d) 200°C.

molded at 200°C do not present any significant variation in the *Tg* values with the addition of up to 60 vol % PS (curve d), whereas *Tg* of PS/EVA18 blends presents a slight increase (curve b). Blends compression-molded at 160°C do not present a significant variation in *Tg* until 40 vol % PS. Beyond this concentration, *Tg* of the EVA phase presents a substantial decrease, which suggests that the mobility of the EVA chains is achieved at lower temperatures as a result of an increase in the free volume of the EVA phase.

Mechanical properties

The Young's modulus (*Ey*) values for PS/EVA18 and PS/EVA28 blends, as obtained from the initial slopes of the stress–strain curves, are plotted as a function of the PS volume fraction and compared to the values predicted with the Takayanagi [eqs. (1) and (2)], Davies , and Budiansky models in Figures 14 and 15. The moduli show a sharp increase when PS becomes continuous throughout the sample. For blends containing around 40 vol % PS, the modulus presents a slight increase in blends mixed and compression-molded at 160°C. At this composition, the PS phase presents a higher continuity degree in blends compression-molded at 160°C, as indicated by selective extraction experiments. Therefore, it seems that PS contributes more to the modulus of the blend when it is more continuous. This feature has also been reported in the literature for other polymer systems.18,22 The moduli of the blends between 50 and 60 vol % PS are quite similar, whatever the processing temperature and EVA sample, because at this composition, all blends present a cocontinuous morphology. Blends containing a low amount of EVA (ca. 20 vol %) present the opposite behavior; that is, those compression-molded at 160°C display lower values of the modulus. These results can be attributed to the higher melt viscosity of the PS matrix at this temperature, which gives rise to a worse dispersion of the EVA domains and consequently poorer mechanical behavior.

It is evident that the *Ey* values show the same behavior as that found for *E'*. The moduli for cocontinuous blends are again higher than the moduli of blends

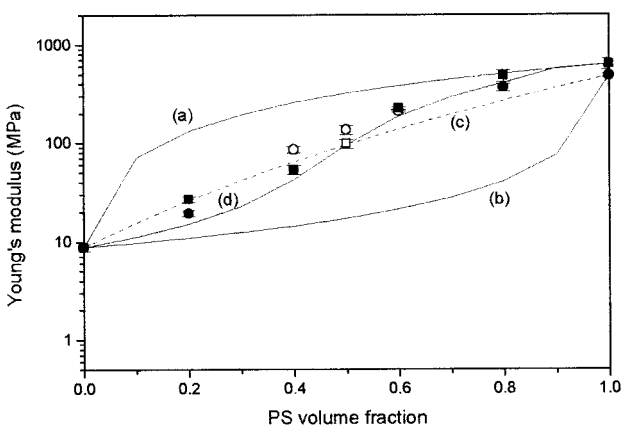

Figure 14 *Ey* values of PS/EVA18 blends as a function of the blend composition in comparison with modulus–composition models: (a) parallel, (b) series, (c) Davies, and (d) Budiansky. The blends were prepared at (●) 160 and (■) 200°C. The open symbols represent cocontinuous morphologies.

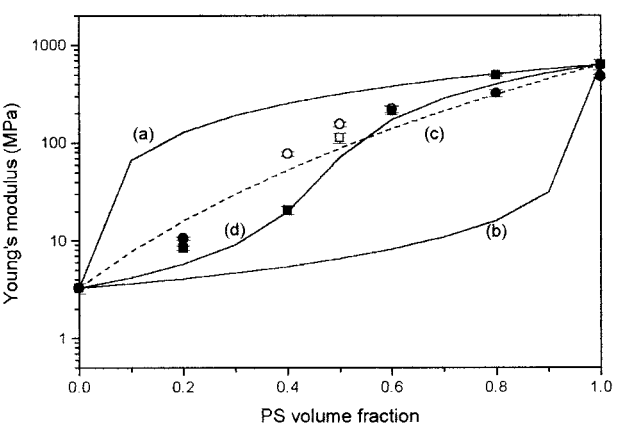

Figure 15 *Ey* values of PS/EVA28 blends as a function of the blend composition in comparison with modulus–composition models: (a) parallel, (b) series, (c) Davies, and (d) Budiansky. The blends were prepared at (●) 160 and (■) 200°C. The open symbols represent cocontinuous morphologies.

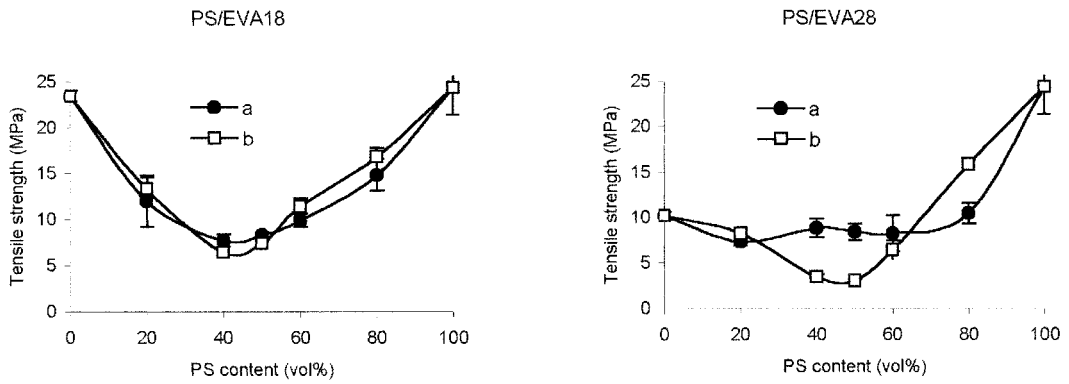

Figure 16 Tensile strength of PS/EVA blends as a function of the blend composition. The blends were compression-molded at (a) 160 and (c) 200°C.

with dispersed morphologies, and a substantial increase in the modulus is found when PS becomes continuous. Theses results are similar to those found by Willemse et al.[21] and Veenstra et al.[16] for PS polymer blends. Concerning the theoretical predictions, the data agree the findings of Hourston and coworkers.[37,38] They observed similar curve shapes for *Ey* and *E′* versus the composition. The values for the latter are higher than the *Ey* values, which are explained by the frequency effect. Moreover, the experimental data of *Ey* fit quite well into the Budiansky model for blends compression-molded at 200°C.

The tensile strength of these blends is illustrated in Figure 16 as a function of the blend composition and molding temperature. No significant difference was found in this property with the molding conditions for PS/EVA18 blends. For PS/EVA28, the EVA28 sample displays a lower tensile strength than EVA18. Therefore, the influence of the cocontinuous morphology achieved in blends compression-molded at 160°C (between 40 and 50 vol % PS) on the tensile strength is more significant.

CONCLUSIONS

The molding temperature substantially affects the range of cocontinuity and the percolation threshold point in PS/EVA blends. These blends are immiscible and present a relatively high interfacial tension. The elongated structures, responsible for the cocontinuous morphology, are nonequilibrium states under quiescent conditions. When they are kept at elevated temperatures, the interfacial area tends to decrease, resulting in an increase in the phase size of the cocontinuous blend or in a breakup of the cocontinuous structure into a droplet–matrix morphology. Therefore, at higher molding temperatures, the range of cocontinuity becomes narrower. The effects of the molding temperature and the characteristics of the EVA sample on the cocontinuity range were also confirmed by SEM micrographs.

PS/EVA18 and PS/EVA28 (60:40 vol %) blends display a cocontinuous morphology, whatever the molding conditions are. However, it is possible to observe from SEM micrographs a coarsening effect with molding at a higher temperature (200°C). Because all blends present dual-phase continuity, there is no substantial influence of the molding conditions or EVA nature on both *Ey* (obtained from stress–strain experiments) and *E′* (obtained from dynamic mechanical analysis).

PS/EVA (40:60 vol %) blends obviously contain a lower amount of the PS phase. Their morphologies change from a cocontinuous structure to a droplet–matrix morphology, depending on the molding conditions and also on the EVA sample, as indicated by selective extraction experiments and SEM analysis. This phenomenon significantly affects the modulus of the blends. *Ey*, obtained from stress–strain measurements, decreases a little when the morphology changes from being cocontinuous to droplet–matrix. The effect of the cocontinuous morphology is more pronounced on *E′* (obtained from DMTA). Blends prepared at 160°C present higher *E′* values, as expected, because of the cocontinuous morphology. These high moduli exceed the values predicted by the Davies model, but for all compositions, the shape of the Budiansky model is quite similar to the experimental data. Changing the structure from droplet–matrix to cocontinuous at a given composition can result in a quite significant increase in the modulus.

References

1. Paul, D. R.; Newman, S. Polymer Blends; Academic: New York, 1978; Vols. 1 and 2.
2. Utracki, L. A. Polymer Alloys and Blends; Hanser: New York, 1989.
3. Favis, B. D.; Chalifoux, J. P. Polymer 1988, 29, 1761.
4. Favis, B. D.; Therriem, D. Polymer 1991, 32, 1474.
5. Lyngaae-Jorgensen, J.; Utracki, L. A. Makromol Chem Macromol Symp 1991, 48, 189.
6. Avgeropoulos, G. N.; Weissert, F. C.; Biddison, P. H.; Böhm, G. G. A. Rubber Chem Technol 1975, 49, 93.

7. Mekhilef, N.; Verhoogt, H. Polymer 1996, 37, 4069.
8. Nelson, C. J.; Avgeropoulos, G. N.; Weissert, F. C.; Böhm, G. G. A. Angew Makromol Chem 1977, 60, 49.
9. Miles, I. S.; Zurek, A. Polym Eng Sci 1988, 28, 796.
10. Utracki, L. A. J Rheol 1991, 35, 1615.
11. Verhoogt, H.; van Dam, J.; Boer, A. P. Adv Chem Ser 1994, 239, 333.
12. Willemse, R. C.; Boer, A. P.; van Dam, J.; Gotsis, A. D. Polymer 1998, 39, 5879.
13. Willemse, R. C.; Boer, A. P.; van Dam, J.; Gotsis, A. D. Polymer 1999, 40, 827.
14. Veenstra, H.; van Dam, J.; Boer, A. P. Polymer 1999, 40, 1119.
15. Veenstra, H.; van Lent, B. J. J.; van Dam, J.; Boer, A. P. Polymer 1999, 40, 6661.
16. Veenstra, H.; van Dam, J.; Boer, A. P. Polymer 2000, 41, 3037.
17. Veenstra, H.; Verkooijen, P. C. J.; van Lent, B. J. J.; van Dam, J.; Boer, A. P.; Nijhof, A. P. H. J. Polymer 2000, 41, 1817.
18. Quintens, D.; Groeninckx, G.; Guest, M.; Aerts, L. Polym Eng Sci 1990, 30, 1484.
19. Harrats, C.; Blacher, S.; Fayt, R.; Jerome, R.; Teyssie, P. J Polym Sci Part B: Polym Phys 1995, 33, 801.
20. Andradi, L. N.; Hellmann, G. P. Polym Eng Sci 1995, 35, 693.
21. Willemse, R. C.; Sperjer, A.; Langeraar, A. E.; Boer, A. P. Polymer 1999, 40, 6645.
22. Mamat, A.; Vu-Khank, T.; Cigana, P.; Favis, B. D. J Polym Sci Part B: Polym Phys 1997, 35, 2583.
23. Gubbels, F.; Blacher, S.; Vanlathem, E.; Jerome, R.; Deltour, R.; Browers, F.; Teyssie, P. Macromolecules 1995, 28, 1559.
24. Soares, B. G.; Gubbels, F.; Jerome, R.; Teyssie, P. H.; Vanlathem, E.; Deltour, R. Polym Bull 1995, 35, 223.
25. Soares, B. G.; Gubbels, F.; Jerome, R.; Vanlathem, E.; Deltour, R. Rubber Chem Technol 1997, 70, 60.
26. Zhang, M. P.; Yu, G. Macromolecules 1998, 31, 6724.
27. Favis, B. D.; Chalifoux, J. P. Polym Eng Sci 1987, 27, 1591.
28. Favis, B. D. Macromol Chem Macromol Symp 1992, 56, 143.
29. Wu, S. Polym Eng Sci 1987, 27, 335.
30. Luzinov, I.; Pagnoulle, C.; Jérôme, R. Polymer 2000, 41, 3381.
31. Brandrup, J.; Immergut, E. H. Polymer Handbook, 3rd ed.; Wiley: New York, 1989; p VI/429.
32. Donateli, A. A.; Sperling, L. H.; Thomas, D. A. Macromolecules 1976, 9, 676.
33. Sperling, L. H. J Polym Sci Part D: Macromol Rev 1977, 12, 141.
34. Fox, R. B.; Bitner, J. L.; Hinkley, J. A.; Carter, W. Polym Eng Sci 1985, 25, 157.
35. Mishra, S. P.; Deopura, B. L. J Appl Polym Sci 1987, 33, 759.
36. Holsti-Miettinem, R. M.; Seppälä, J. V. Polym Eng Sci 1994, 34, 395.
37. Hourston, D. J.; Schäfer, F.-U. Polymer 1996, 37, 3521.
38. Hourston, D. J.; Schäfer, F.-U.; Grandwell, M. H. S.; Song, M. Polymer 1998, 39, 5609.
39. Nielsen, L. E. Mechanical Properties of Polymers and Composites; Marcel Dekker: New York, 1974; Vols. 1 and 2.
40. Kerner, E. H. Proc Phys Soc London Sect B 1956, 69, 808.
41. Davies, W. E. A. J Phys D: Appl Phys 1971, 4, 1176.
42. Davies, W. E. A. J Phys D: Appl Phys 1971, 4, 1325.
43. Budiansky, B. J Mech Phys Solids 1965, 13, 223.
44. McCrum, N. G.; Buckley, C. P.; Bucknall, C. B. Principles of Polymer Engineering; Oxford University Press: Oxford, England, 1989.
45. Hahnfeld, J. L.; Dalke, B. D. In Encyclopedia of Polymer Science and Engineering, 2nd ed.; Mark, H. F.; Bikales, N. M.; Overberger, C. G.; Menges, G., Eds.; Wiley: New York, 1989; Vol. 16.
46. Dedecker, K.; Groeninckx, G. Polymer 1998, 39, 4993.